Petrogenesis of the Platreef, Bushveld Complex, South Africa interrogated using mass-independent sulfur isotopes

Sarah C. Penniston-Dorland, Boswell A. Wing, Michael Brown, and Margaret A. Baker

Department of Geology, University of Maryland, College Park, MD 20742

Report for the USGS Mineral Resources External Research Program

(USGS Grant #05HQGR0158)

Introduction

The Bushveld Complex, which underlies an area of more than 66,000 km^2 in northeastern South Africa, is the world's largest layered igneous intrusion; it hosts many economically important ores: copper, tin, chromium, gold, vanadium, and platinum-group metals. According to the U.S. Geological Survey (USGS) Mineral Commodity Summaries, January 2007, South Africa hosts close to 89% of the world's platinum-group metal reserves, with the Bushveld Complex serving as the largest single reserve.

The Bushveld Complex consists of three major regions: the Eastern and Western Lobes, and the Northern Limb (Figure 1). In the Eastern and Western lobes the mineralization is hosted in the interior of the Complex, in the Merensky Reef and UG2 Chromitite layers. The contact relationships of these mineralized layers with the host igneous rocks are non-transgressive, and the source of mineralization is believed to be primarily magmatic. In contrast, in the Northern limb, the mineralization is hosted at the lower margin of the Complex, in the Platreef. The contact relationships of the Platreef are transgressive with the underlying footwall rocks, and the possibility of a non-magmatic component to the source of ore elements/minerals is debated. There are abundant footwall-derived xenoliths in the Platreef and mineral textures suggestive of magma-footwall reaction at the contact. These features suggest that platinum-group metals and associated sulfides may be at least partly derived from the underlying footwall rocks.

Our research tests the hypothesis that sulfur in the Platreef was derived from the underlying footwall rocks. We use mass-independently fractionated sulfur isotopes ($\Delta^{33}S$) to track ore-forming processes in the Platreef. This approach represents a new application of a recently developed isotopic tracer.

Some of the footwall rocks surrounding the Platreef are older than 2.45 Ga. Rocks of this

age that were exposed to the atmosphere (e.g. sedimentary rocks) should record mass-independent (non-zero) values of $\Delta^{33}S$. If the Bushveld magma was mantle-derived, it should record mass-dependent ($\Delta^{33}S$ <0.2‰) $\Delta^{33}S$. If these assumptions hold true, then according to the hypothesis we have proposed samples from the Platreef should record $\Delta^{33}S > 0.2$‰, indicating interaction of magma with the underlying footwall rocks.

Geologic Background

The layered mafic-ultramafic rocks of the Bushveld Complex have been designated the Rustenberg Layered Suite (RLS). The RLS intruded into the Transvaal Supergroup sedimentary rocks (Figure 1) at 2.06 Ma (U-Pb titanite date, Buick et al., 2001). The RLS is commonly divided (from bottom to top) into the Marginal, Lower, Critical, Main, and Upper Zones (see Cawthorn and Walraven (1998) for descriptions). The focus of this study is a part of the northern limb in which only the Main and Upper Zones are present, underlain by the Platreef ore horizon. The Lower Zone is expressed in the northern limb further to the south of the study area and in several large satellite bodies in the area, but the Critical Zone is poorly developed in the northern limb (Gain and Mostert, 1982). The sedimentary rocks of the Transvaal Supergroup into which the RLS intrudes were deposited from ~2.6 to 2.3 Ga (Bekker *et al.,* 2001, 2004; Hannah et al., 2004; Figure 2).

The Platreef is composed of medium to coarse-grained pyroxenites and norites. Previous researchers have noted an abundance of dolomite xenoliths in the Platreef—ranging in size from a few centimeters to 90 m in diameter—and hypothesized that the xenoliths are evidence for interaction between the local footwall rock and the magma in the Platreef (Buchanan *et al.,* 1981; Gain and Mostert, 1982; Cawthorn *et al.,* 1985; Barton *et al.,* 1986; Harris and Chaumba, 2001).

The contact between the RLS and footwall rocks in the northern limb is transgressive, with the Platreef in contact with progressively older rocks of different lithologies from south to north (see Figure 3). The Platreef is a highly geochemically variable unit, and detailed studies suggest that lateral variations in the geochemistry of the Platreef are the result of interaction with and incorporation of different types of footwall rock (Holwell and McDonald, 2006).

Traditional sulfur isotope measurements ($\delta^{34}S$) on sulfides from the Bushveld yielded a range of $\delta^{34}S$ from -0.6 to 3.5‰ (Buchanan *et al.*, 1981). Traditional sulfur isotope compositions of sulfides from the Platreef (Buchanan *et al.,* 1981; Manyeruke *et al*., 2005; Sharman-Harris *et al.*, 2005) range from ~+3 up to ~+10‰, with the higher values attributed to incorporation of the material from the footwall.

Geochemistry of multiple sulfur isotopes

Current theory and observation demonstrate that solid-earth geological processes that fractionate sulfur isotopes produce the following relationship: $\delta^{33}S \sim 0.515 \times \delta^{34}S$ (Hulston and Thode, 1965; Farquhar and Wing, 2003; Fig. 4), where the δ notation expresses the relative deviation of a measured isotope ratio from a reference isotope ratio (e.g., $\delta^{34}S = [^{34}S/^{32}S]_{meas} / [^{34}S/^{32}S]_{ref} - 1$; all values shown here are referenced to V-CDT and expressed in permil, ‰). Sulfur isotope compositions from a range of sulfides and sulfates older than *ca*. 2450 Ma, however, do not follow these linear 'mass-dependent' relationships and yield anomalous, 'mass-independent' values that are quantified by $\Delta^{33}S \sim \delta^{33}S_{meas} - 0.515 \times \delta^{34}S_{meas}$ (Farquhar *et al*., 2000; Figs. 4 and 5). The tildes indicate that these linear relationships are only approximate because of the exponential dependence of isotope fractionation on mass. The linearized relationships are for illustration only and all values shown here are calculated without approximation (see Table 1).

Practically speaking, $\Delta^{33}S$ and $\Delta^{36}S$ have definitions that depend on $\delta^{34}S$, with mass-dependent processes able to cause variations in $\Delta^{33}S$ of about 0.01‰ for every permil variation in $\delta^{34}S$. Production of non-zero $\Delta^{33}S$ outside this range has only been experimentally verified through the irradiation of common gas-phase sulfur-bearing molecules, such as SO_2 and H_2S, with short wavelength ultraviolet light (Farquhar *et al*., 2000; 2001). Because current evidence places the process of mass-independent fractionation exclusively in the gas phase, any sulfur in a solid compound that now exhibits non-zero $\Delta^{33}S$ has spent a portion of its lifetime in the atmosphere, most likely bound up in SO_2 or H_2S. The presence of non-zero $\Delta^{33}S$ in terrestrial sulfides and sulfates, therefore, is a direct indication that a portion of their sulfur has been processed through the surface environment on early Earth.

Scientific effort so far has been largely directed towards documenting and expanding the primary record of mass-independent sulfur isotope fractionation by analyzing Archean and Paleoproterozoic sedimentary sulfides and associated sulfates (Ono *et al*., 2003; Mojzsis *et al*., 2003; Bekker *et al*., 2004). The existence of a single, atmospheric source for mass-independently fractionated sulfur isotopes, however, means that $\Delta^{33}S$ is a chemically conservative tracer of surface sulfur as it passes through solid-earth geological processes. The conservative nature of $\Delta^{33}S$ has been exploited in a number of studies that trace surface sulfur through the geologic branches of the global sulfur cycle. For example, measurements from sulfide inclusions in diamonds have identified Archean sedimentary sulfur in the source regions of Paleoproterozoic diamonds (Farquhar *et al*., 2002), and mass-independently fractionated sulfur isotopes in ore sulfides from many Archean volcanic massive sulfide deposits document the hydrothermal transfer of sulfur from the Archean surface sulfate reservoir (Jamieson *et al.,* 2006). Despite the potential usefulness to many ore-forming processes, $\Delta^{33}S$ has not yet been applied as a

conservative tracer of surface sulfur on the scale of a single ore deposit.

In an environment like the Platreef, $\Delta^{33}S$ measurements are uniquely suited to trace the evolution of sulfur through the ore-forming process. The Transvaal Supergroup footwall rocks and the Platreef were formed during a critical time interval in which there is a transition from older rocks (>2.45 Ga) that record non-zero $\Delta^{33}S$ (mass-independent or anomalous fractionation) to younger rocks (<2.0 Ga) that record mass-dependent fractionation ($\Delta^{33}S = 0 \pm 0.2‰$) (see Figure 5). The Bushveld Complex itself is a mafic intrusion that is primarily mantle-derived. It should record mass-dependent sulfur isotope fractionation ($\Delta^{33}S = 0‰$). Measured $\Delta^{33}S$ in some of the older footwall rocks are hypothesized to be non-zero, in which case the non-zero values of $\Delta^{33}S$ can potentially be traced into the Bushveld Complex if any of the sulfur in the Platreef is derived from the footwall rocks.

Approach

A geologic sketch map in Figure 3 shows the locations of boreholes from which most of the samples were collected for sulfur isotope analysis.

Reconstruction of the sulfur multiple-isotope stratigraphy of unmetamorphosed equivalents of Platreef footwall rocks

Sedimentary equivalents to the rocks in the Platreef footwall were deposited from *ca*. 2600 Ma to *ca*. 2300 Ma (Bekker *et al.,* 2001; 2004; Hannah *et al.,* 2004), which spans the abrupt diminution of the mass-independent sulfur isotope signal at *ca*. 2450 Ma (Farquhar *et al.*, 2000; Fig. 5). A pronounced unconformity exists between the Penge Iron Formation–Tongwane Formation and the overlying Duitschland Formation that may represent *ca*.100 Ma in missing

time (Eriksson *et al.,* 2001; Bekker *et al*., 2004). Recent sulfur multiple-isotope measurements on samples from the lower part of the Timeball Hill Formation and the underlying Rooihoogte Formation (approximately equivalent to the Duitschland Formation) have been interpreted as mass-dependent (Bekker *et al.,* 2004). Taken together, these lines of evidence suggest that any sizable non-zero $\Delta^{33}S$ in sulfur in the Platreef footfootwall will be confined to the Penge Iron Formation and the Malmani Dolomite Formation. Observations of a uniformly negative $\Delta^{33}S$ in sulfides associated with Archean Dolomites from the Hamersley Basin (Ono *et al.,* 2003) and in Archean barites worldwide (Farquhar *et al.,* 2000) further suggest that the $\Delta^{33}S$ of sulfur associated with the Malmani Dolomite Formation is likely to be negative. We tested these preliminary hypotheses by measuring the sulfur multiple-isotope compositions of sulfide and sulfate in a representative suite of samples from unmetamorphosed equivalents to the rocks of the Platreef footfootwall.

Characterization of the sulfur multiple-isotope composition of Platreef magmatic sulfur and ore sulfides

Magmatic sulfur

Isotope fractionation theory and measurements from meteorites (e.g., Gao and Thiemens, 1993) and peridotite xenoliths (e.g., Farquhar *et al.*, 2002) suggest that 'primary' igneous sulfur will exhibit a mass-dependent isotopic composition (i.e., $\Delta^{33}S \sim 0$). Therefore, we made the null hypothesis that any primary igneous sulfur in the Platreef ore sulfides will have sulfur multiple-isotope compositions characterized by $\delta^{34}S \sim 0$ and $\Delta^{33}S \sim 0$. This null hypothesis cannot be tested directly in the Platreef because of probable assimilation of footfootwall sulfur, which may lead to non-zero $\Delta^{33}S$ values. We have tested this hypothesis indirectly by measuring the sulfur

multiple-isotope composition of sulfides from five different samples, including barren feldspathic pyroxenites at the contact of the Platreef with the lowermost Main Zone of the RLS and norites from the Main Zone. Although there are only trace amounts of sulfides in these rock types (Armitage *et al*., 2002), their sulfur multiple-isotope compositions may provide our best local approximation of the isotopic composition of the sulfur in the parental Platreef magma. Even if the null hypothesis fails, the analyses will establish a reference sulfur multiple-isotope end member for the Platreef magma. This reference composition is necessary to quantify how much, if any, mass-independently fractionated sulfur was incorporated into the Platreef from its footfootwall.

Ore sulfides and sulfur source

If ore sulfides were crystallized directly from pristine Platreef magma, they should record the same range of values of $\Delta^{33}S$ as the pristine magma. On the other hand, if they were crystallized from magma that interacted with footwall rock during emplacement, the potential for mass-independent values of $\Delta^{33}S$ exists.

Samples with the same $\Delta^{33}S$ share the same sulfur source; mass-dependent fractionation processes (i.e., fractional crystallization, equilibrium isotope exchange) acting on a single mass-independent source will simply lead to a secondary fractionation array parallel to the mass-dependent line in figure 4. The offset between the secondary fractionation array and the mass dependent array passing through the origin quantifies the mass-independent signature of the source. Therefore, different ore sulfides in close proximity may have crystallized from the same sulfur source, in which case their $\Delta^{33}S$ values are likely to be the same, despite having variable $\delta^{34}S$ values. We have examined the question of sulfur source by measuring the sulfur multiple-

isotope compositions of Platreef coexisting ore sulfides.

Dependence of mineralization on footwall rock

Observations of the dependence of mineralization on the rock type in the Platreef footwall (Viljoen and Schürmann, 1998) suggest that $\Delta^{33}S$ in ore sulfides may vary in concert with footwall rock type. To this end, samples were collected from two cores, one with carbonate footwall and one with pelite footwall. The sulfur isotopic composition was measured on samples taken from closely spaced intervals along the cores near the contact between Platreef and footwall rock (~1-5 m spacings) and more spread out further away from the contact (~50 m spacing).

Methods

Whole rock samples were pulverized and reacted with a Cr-reducing solution, liberating H_2S, which was then trapped using a zinc acetate solution and reacted with $AgNO_3$ to produce Ag_2S. The Ag_2S was converted to SF_6 by reaction with an excess of F_2 at 250 °C for 8 h in a Ni reaction vessel. Separated sulfide minerals were heated using a CO_2 laser, reacted with F_2 gas and directly converted to SF_6. In both cases, the resulting SF_6 was condensed from the residual F_2 into a liquid-nitrogen cooled trap (-177 °C), and subsequently distilled from a trap at 115 °C to the injection loop of a gas chromatograph (GC) at -177 °C. GC purification of SF_6 was undertaken using a 1/8 in. diameter, 12 foot long column with a He carrier flow at 20 mL/min. The SF_6 peak was registered on a TCD and then isolated by freezing into a liquid-nitrogen cooled trap. Purified SF_6 was introduced into the ThermoFinnigan MAT 253 dual-inlet gas-source mass spectrometer at the University of Maryland and sulfur isotope abundances were

measured by monitoring the $^{32}SF_5^+$, $^{33}SF_5^+$, and $^{34}SF_5^+$ ion beams at m/z = 127, 128, and 129.

Reproducibility of the measurement procedures was monitored using three different standards. Multiple measurements (n=8) of a well-characterized silver sulfide standard (using the method of conversion to SF_6 in a Ni reaction vessel) indicate that $\delta^{34}S$ was measured with an external reproducibility of ±0.29‰ (1σ) and $\delta^{33}S$ with an external reproducibility of ±0.14‰ (1σ). Similar tests for $\Delta^{33}S$ yield a reproducibility of ±0.02‰ (1σ). Multiple measurements (n=3) of an internal pyrite standard were made using the laser heating method. The external reproducibility of these measurements for $\delta^{34}S$ was ± 0.09‰ (1σ), ±0.04‰ for $\delta^{33}S$ (1σ), and ±0.02‰ for $\Delta^{33}S$ (1σ). Finally, a sample of sulfide-bearing Platreef pyroxenite was pulverized and aliquots of this powder were reacted and analyzed multiple times (n=5) to determine reproducibility of the entire process of chemical extraction and analysis. The reproducibility of these measurements was similar to those for the silver sulfide standard: ±0.29‰ for $\delta^{34}S$ (1σ), ±0.15‰ for $\delta^{33}S$ (1σ), and 0.01‰ for $\Delta^{33}S$ (1σ).

Results

Reconstruction of the sulfur multiple-isotope stratigraphy of unmetamorphosed equivalents of Platreef footwall rocks

Twenty-one samples of the unmetamorphosed equivalents to Platreef wall rocks were analyzed for their sulfur multiple isotope composition (Table 2). The isotopic composition of the operationally-defined sulfide pool was measured from shale samples, while the operationally-defined sulfate pool was measured from carbonate (limestone, dolostone) samples. Sulfur multiple isotope compositions of unmetamorphosed equivalents to Platreef footwall rocks exhibit a stratigraphic dependence, with rocks lower in the stratigraphy (Malmani Dolomite, lower

Duitschland Formation) characterized by mass-independent sulfur isotope fractionation ($\Delta^{33}S$ values up to 2.8‰) and $\delta^{34}S$ values from ~ -1.5‰ to ~14.5‰. The highest $\delta^{34}S$ values were measured in carbonate-associated sulfate from the Malmani Dolomite. Samples from higher in the stratigraphy have near zero $\Delta^{33}S$ values (<0.2‰) and $\delta^{34}S$ values from ~16.1‰ to ~42.3‰. This range in isotopic composition provides a natural framework for tracing the movement of sulfur between the Platreef and its wall rocks.

Establishment of the sulfur multiple-isotope composition of Platreef magmatic sulfur and ore sulfides

Magmatic sulfur

A suite of samples that were chosen as proxies for the primary Platreef magma was analyzed for sulfur isotopic composition. Two samples (N6.2, BHTv11; Nex *et al.*, 2002) were selected from Main Zone rocks of the western Bushveld Complex. Two samples of feldspathic pyroxenite (P3-MZLo, P3-MZHi) were collected from the Main Zone of the RLS near its lower contact with the Platreef. One additional sample (C2-20) was collected from unmineralized Platreef pyroxenite near its upper contact with the Main Zone.

The measured values for $\delta^{34}S$ range from +1.3 to 3.2 ‰ (Table 1, Figure 6). Some of these values are slightly higher than the measured range of $\delta^{34}S$ in meteorites, believed to represent the sulfur isotopic composition of the mantle (0 ± 2‰; Thode et al., 1961) and slightly higher than values reported for mid-ocean ridge basalts (-0.3 ± 2.3‰) but fall within error of the range for ocean island basalts (1.0 ± 1.9‰) (see Seal, 2006 for review).

The measured values of $\Delta^{33}S$ fall between +0.11 and +0.21‰ (Table 1, Figure 6). Whether these measurements are mass-dependent is open to interpretation. A compilation of 123

mass-dependent measurements (age < 2.0 Ga) reveals a range of $\Delta^{33}S$ values from -0.11 to +0.25‰. When the measured values are plotted on a graph of $\delta^{33}S$ vs. $\delta^{34}S$, however, the points all plot on a line above the range of lines with mass-dependent slopes (0.5 to 0.516) and a zero intercept, on a line with slope of 0.51 and a non-zero intercept (+0.12‰). This is suggestive of mass-dependent fractionation of a source that may have had a mass-independent component. This could be explained by interaction of the Bushveld magma with deeper-seated footwall rocks. Interaction of Bushveld magma with lower to middle crust has been proposed by Harris *et al.,* (2005) based on oxygen isotope compositions of mineral separates that indicate a magma with an oxygen isotopic composition higher than that of the mantle. More work needs to be done to characterize the sulfur isotope composition of unmineralized pristine Bushveld Complex igneous rock to determine whether the sulfur isotope composition of these rocks supports this conclusion.

Ore sulfides and sulfur source

Samples from six different drill cores through the Platreef were analyzed for sulfur multiple isotope composition. Figure 7 shows the sulfur isotopic compositions of all the samples analyzed from the Platreef ore horizon from these cores (see Figure 3 for borehole locations). The results show values of $\delta^{34}S$ ranging from ~+2 up to ~+13‰ and values of $\Delta^{33}S$ ranging from near zero up to +0.55‰. There are twelve analyses that are clearly mass-independent, that is they fall outside of error of the range of mass-dependent sulfur isotope compositions ($\Delta^{33}S < 0.2$‰).

For this study, mineral phases from the same hand sample (~5 cm length pieces of core) were considered to be coexisting phases. Sulfide minerals were separated by handpicking with a magnet to determine whether different sulfide phases had the same sulfur source and whether they were in equilibrium. Mineral separates of chalcopyrite (Ccp) and pyrrhotite (Po) were

examined using back-scattered electron imaging and qualitative energy dispersive spectrometer analyses on the JEOL JXA-8900 electron probe microanalyzer at the University of Maryland for three of the six samples analyzed. In most samples, the grains separated as Po appeared to be ≥ 90% Po with very small quantities of pentlandite (Pn). Coexisting sulfides in equilibrium should have $\delta^{34}S$ values that correspond to predicted equilibrium fractionation of ^{34}S and ^{32}S between sulfide minerals ($\delta^{34}S_{Ccp} < \delta^{34}S_{Po} \approx \delta^{34}S_{Pn}$, Ohmoto and Rye, 1979).

Measured values of $\Delta^{33}S$ for all but one set of coexisting sulfide separates are consistent with single $\Delta^{33}S$ values (Table 3, Figure 8), suggesting that the phases within these samples share the same source of sulfur. In one sample, however, (C1-19) the measured $\Delta^{33}S$ was distinctively higher in the Po fraction than in the Ccp fraction, suggesting a different source of sulfur for each mineral phase. In some coexisting sulfide separates measured values of $\delta^{34}S_{Ccp}$ are less than measured values of $\delta^{34}S_{Po}$ and in others the relationship is the reverse (Table 3, Figure 9). This suggests that at least some of the samples are not consistent with equilibrium fractionation of $^{34}S/^{32}S$.

Dependence of mineralization on footwall rock

Samples from detailed profiles along the length of two cores drilled through the Platreef into underlying footwall rock were collected and analyzed as bulk sulfide to test for the control of the type of footwall rock on the sulfur isotope composition of the Platreef. One core had carbonate footwall (C1) and the other had pelitic footwall (P1) (see Figure 3).

In core C1 the thickness of the Platreef is ~150 m and in core P1 the Platreef thickness is ~225 m. In core P1 the footwall rock extends for ~70 m through hornfels (likely metamorphosed lower Duitschland Formation) together with some calc-silicate rock and at the base into a banded

iron formation (likely the Penge Iron Formation). In core C1 the footwall rock extends for 143 m through calcsilicate rock (likely metamorphosed Malmani Dolomite Formation).

In both cores the Platreef rocks include pyroxenite, feldspathic pyroxenite, and norite; the main sulfide phases are pyrrhotite, pentlandite and chalcopyrite. The mineralogy of the carbonate footwall rock in core C1 includes calcite, dolomite, rhodochrosite, forsterite, diopside, brucite pseudomorphs after periclase, and magnetite, and sulfide phases include pyrrhotite, pyrite, and alabandite. The mineralogy of the pelitic footwall rock in core P1 includes quartz, biotite, muscovite, garnet, plagioclase, amphibole, ilmenite, and magnetite, and the main sulfide phases are pyrrhotite and chalcopyrite.

The measured sulfur isotopic compositions for both traverses are reported in Tables 4 and 5 and Figures 10 and 11. In both cores the measured $\Delta^{33}S$ is relatively low in the upper parts of the Platreef (upper parts of the cores), with values that fall within error of the range of the measured values for relatively pristine igneous rocks. In both cores the measured $\Delta^{33}S$ is relatively high in the footwall rock (lower parts of the cores) with values that can clearly be called mass-independent ($\Delta^{33}S$ = up to 0.9‰ in P1 and up to 5.0‰ in C1). The transition downwards through both cores is a smooth profile that increases downwards into the footwall rock with an inflection point in the footwall.

In the carbonate core (C1) there are measured $\Delta^{33}S$ values in the lower part of the Platreef near the contact with the footwall rock that are outside the range of values normally considered "mass-dependent" ($\Delta^{33}S$ ranges up to 0.55‰). Measured compositions in the Platreef in core P1 are within error of the range of mass-dependent sulfur ($\Delta^{33}S$ ranges up to 0.23‰).

Discussion

As predicted from their depositional ages, the Malmani Dolomite and Lower Duitschland Formation contain sulfur characterized by mass-independent isotope fractionation. Sulfur from the Upper Duitschland Formation, on the other hand, is mass-dependently fractionated. This difference enables a dominant source of sulfur in the Platreef ore horizon to be identified. Non-zero $\Delta^{33}S$ values in samples from the northernmost boreholes require the addition of sulfur from the Malmani Dolomite and/or the Lower Duitschland Formation. This broad correlation between mass-independent fractionation in sulfur isotopes from the Platreef and the underlying wall rock suggest that sulfur movement is largely a local process.

Relatively pristine igneous rocks from the Platreef and Main Zone have sulfur isotope compositions that fall within the range of mass-dependent values ($\Delta^{33}S \leq 0.2‰$) observed in the rock record and that are expected from rocks derived from the mantle. These values are all in the upper part of the mass-dependent range of values, which is suggestive of interaction of the magma with sedimentary rocks that record mass-independent fractionation deeper in the crust.

Measurements on coexisting sulfide phases have implications for the sulfur source and for the cooling history of the system. Analytically indistinguishable $\Delta^{33}S$ isotope compositions of coexisting sulfide phases in individual samples suggests that the sulfur source for the different phases within each sample is the same. Inconsistent fractionation of $\delta^{34}S$ between coexisting sulfide phases in individual samples indicates that there is non-equilibrium distribution of sulfur isotopes between phases, suggesting that different phases closed to sulfur isotope exchange at different temperatures during the cooling of the system.

The detailed measurements of sulfur isotope compositions on rocks of the Platreef and its footwall rocks provide some insight into the processes involved in the formation of the ore

horizon. First, mass-independent sulfur isotope compositions measured in igneous rocks of the Platreef (measured $\Delta^{33}S$ ranges up to 0.55‰) suggest interaction with footwall rocks that record mass-independent sulfur isotope compositions. Second, the mass-independent sulfur isotope compositions recorded in the Platreef are elevated adjacent to the contact with footwall rocks, suggesting local interaction with footwall rock. Third, the size of the mass-independent signature found in the Platreef samples varies depending on the type of footwall rock. All these lines of evidence suggest that there is local interaction between Platreef magma and footwall rock.

The observed smooth increase in $\Delta^{33}S$ across the contact between the Platreef and footwall in both cores is suggestive of an advective-diffusive exchange of sulfur. A model of advection and diffusion has been fit to the curves from both of the detailed core traverses. The average dip of the contact between the Platreef and the footwall rocks is 45 degrees to the west (Gain and Mostert, 1982), so distances from the contact were adjusted for a 45 degree angle. Figures 12 and 13 show the adjusted distances and sulfur isotope compositions along with the modeled fits for both traverses. The best fits for these traverses suggest advection of the sulfur isotope front between 19 and 24 m downwards from the contact. The diffusive exchange of sulfur that accompanied advection is modeled using values of $\sqrt{Dt}$ = 7.7 m (core C1) and 10 m (core P1). The medium for diffusion and outward advection of sulfur was likely an aqueous fluid. Concentration of sulfide phases in veinlets within the footwall rocks supports the hypothesis of outward advection of a sulfur-bearing fluid.

The observed sulfur isotopic compositions can be explained in the context of current models of PGE deposit formation (e.g. Naldrett, 2004) and more specifically in the context of models of Platreef mineralization from a cooling and crystallizing sulfide-rich magma that had assimilated some footwall rock (Buchanan *et al.,* 1981; Gain and Mostert, 1982; Cawthorn *et al.,*

1985; Holwell and McDonald, 2006; Holwell *et al.*, 2006; Holwell and McDonald, 2007). The multiple sulfur isotope data suggest that assimilation of footwall rock occured locally (e.g. Schiffries and Rye, 1989; Harris and Chaumba, 2001), although there may also have been assimilation of footwall rock at a deeper level in the crust (e.g. Harris *et al.,* 2005). As the magma cooled, it became saturated in sulfur and an immiscible sulfide liquid separated from the silicate magma. Sulfide phases crystallized from the immiscible sulfide liquid; first a mono-sulfide solution crystallized (mss) which later exsolved pyrrhotite and pentlandite as intergrown phases. The crystallization of mss increased the concentration of copper in the sulfide melt, and eventually chalcopyrite crystallized.

As the magma continued to cool, an aqueous fluid was exsolved (e.g. Armitage *et al.,* 2002; Hutchinson and Kinnaird, 2005; Holwell *et al.,* 2006). Sulfur in the aqueous fluid had a mass-dependent sulfur isotope composition. The aqueous fluid was advected away from the cooling magma, outward into the surrounding footwall rock. There was a discontinuity in the sulfur isotope composition between sulfur in the distal footwall rock (mass-independent $\Delta^{33}S$) and sulfur in the aqueous fluid (near-zero $\Delta^{33}S$). Exchange of sulfur isotopes by diffusion within the aqueous fluid smoothed out the sharp discontinuity in sulfur isotope composition, creating the observed sulfur isotope profile. As the fluid cooled, it interacted with the rock it was traveling through, and either exchanged sulfur with existing sulfide phases or new sulfide phases crystallized by reaction of sulfur in the fluid with iron in the footwall rock, with different sulfide phases crystallizing depending on the type of footwall rock.

References

Armitage, P.E.B., McDonald, I., Edwards, S.J., and Manby, G.M., 2002. Platinum-group element mineralisation in the Platreef and calc-silicate footfootwall at Sandsloot, Potgietersrus District, South Africa. Transactions of the Institute of Mining and Metallurgy 111, 36-45.

Barton, J.M., Cawthorn, R.G., and White, J., 1986. The role of contamination in the evolution of the Platreef of the Bushveld Complex. Economic Geology 81, 1096-1104.

Buchanan, D.L., Nolan, J., Suddaby, P., Rouse, J.E., and Viljoen, M.J., Davenport, W.J., 1981. The genesis of sulfide mineralization in a portion of the Potgietersrus Limb of the Bushveld Complex. Economic Geology 76, 568-479.

Buchanan, D.L., and Rouse, J.E., 1982. Role of contamination in the precipitation of sulfides in the Platreef of the Bushveld Complex. In: Sulfide deposits in mafic and ultramafic rocks (D.L. Buchanan and M.J. Jones, eds.): Proceedings of IGCP Projects 161 and 91, The Institution of Mining and Metallurgy: London, 141-146.

Buick, I.S., Maas, R., and Gibson R., 2001. Precise U–Pb titanite age constraints on the emplacement of the Bushveld Complex, South Africa. Journal of the Geological Society, London 158, 3-6.

Bekker, A., Kaufman, A.J., Karhu, J.A., Beukes, N.J., Swart, Q.D., Coetzee, L.L., and Eriksson, K. A., 2001. Chemostratigraphy of the Paleoproterozoic Duitschland Formation, South Africa: Implications for coupled climate change and carbon cycling. American Journal of Science 301, p.261-285.

Bekker, A., Holland, H. D., Wang, P.-L., Rumble, III, D., Stein, H.J., Hannah, J.L., Coetzee, L.L., and Beukes, N.J., 2004. Dating the rise of atmospheric oxygen. Nature, 427, p. 117-120.

Cawthorn, R.G., Barton, J.M. and Viljoen, M.J., 1985. Interaction of floor rocks with the Platreef on Overysel, Potgietersrus, Northern Transvaal. Economic Geology 80, 988-1006.

Cawthorn, R. G., and Walraven, F., 1998. Emplacement and crystallization time for the Bushveld Complex. Journal of Petrology, 39, 1669-1687.

Chaussidon, M., Albarède, F., and Sheppard, S.M.F.,1989. Sulphur isotope variations in the mantle from ion microprobe analyses of micro-sulphide inclusions. Earth and Planetary Science Letters, 92, 144-156.

Eriksson, P.G., Altermann, W., Catuneanu, O., van der Merwe, R., and Bumby, A.J., 2001. Major influences on the evolution of the 2.67-2.1 Ga Transvaal basin, Kaapvaal craton. Sedimentary Geology 141, 205-231.

Farquhar, J., Bao, H.M., and Thiemens, M., 2000. Atmospheric influence of earth's earliest sulfur cycle. Science, 289, 756-758.

Farquhar, J., Savarino, J., Airieau, S., and Thiemens, M.H., 2001. Observation of wavelength-sensitive mass-independent sulfur isotope effects during SO_2 photolysis: Implications for the early atmosphere. Journal Geophysical Research 106, 32829-32839.

Farquhar, J., Wing, B.A., McKeegan, K.D., Harris, J.W., Cartigny, P., and Thiemens, M.H., 2002. Mass-independent sulfur of inclusions in diamond and sulfur recycling on early Earth. Science 298, 2369-2372.

Farquhar, J., and Wing, B.A., 2003. Multiple sulfur isotopes and the evolution of the atmosphere. Earth and Planetary Science Letters 213, 1-13.

Gain, S.B., and Mostert, A.B., 1982. The geological setting of the platinoid and base metal sulfide mineralization in the Platreef of the Bushveld Complex in Drenthe, north of Potgietersrus. Economic Geology 77, 1395-1404.

Gao, X., Thiemens, M.H., 1993. Variations of the isotopic composition of sulfur in enstatite and ordinary chondrites. Geochimica et Cosmochimica Acta, 57, 3171-3176.

Hannah, J.L., Bekker, A., Stein, H.J., Markey, R.J., and Holland, H.D., 2004. Primitive Os and 2316 Ma age for marine shale: implications for Paleoproterozoic glacial events and the rise of atmospheric oxygen. Earth and Planetary Science Letters, 225, 43-52.

Harris, C., and Chaumba, J.B., 2001. Crustal contamination and fluid-rock interaction during the formation of the Platreef, northern lobe of the Bushveld intrusion, South Africa. Journal of Petrology, 42, 1321-1347.

Harris, C., Pronost, J.J.M., Ashwal, L.D., and Cawthorn, R.G., 2005. Oxygen and hydrogen isotope stratigraphy of the Rustenberg Layered Suite, Bushveld Complex: Constraints on crustal contamination. Journal of Petrology, 46, 579-601.

Holwell, D.A., and McDonald, I., 2006. Petrology, geochemistry and the mechanisms determining the distribution of platinum-group element and base metal sulphide mineralisation in the Platreef at Overysel, northern Bushveld Complex, South Africa. Mineralium Deposita, 41, 575-598.

Holwell, D.A., McDonald, I., and Armitage, P.E.B., 2006. Platinum-group mineral assemblages in the Platreef at the Sandsloot Mine, northern Bushveld Complex, South Africa. Mineralogical Magazine, 70, 83-101.

Holwell, D.A., and McDonald, I., 2007. Distribution of platinum-group elements in the Platreef at Overysel, northern Bushveld Complex: a combined PGM and LA-ICP-MS study. Contributions to Mineralogy and Petrology, 154, 171-190.

Hu, G., Rumble, D., and Wang, P.-L., 2003. An ultraviolet laser microprobe for the *in situ* analysis of multisulfur isotopes and its use in measuring Archean sulfur isotope mass-independent anomalies. Geochemica et Cosmochimica Acta, 67, 3101-3118.

Hulston, J.R., and Thode, H.G., 1965. Variations in ^{33}S, ^{34}S and ^{36}S contents of meteorites and their relation to chemical and nuclear effects. Journal of Geophysical Research 70, 3475-3484.

Hutchinson, D., and Kinnaird, J.A., 2005. Complex multistage genesis for the Ni-Cu-PGE mineralisation in the southern region of the Platreef, Bushveld Complex, South Africa. Applied Earth Science: Transactions of the Institute for Mining Metallurgy B, 114, B208-B224.

Jamieson, J. W., Wing, B. A., Hannington, M.D., and Farquhar, J., 2006. Evaluating isotopic equilibrium among sulfide mineral pairs in Archean ore deposits: Case study from the Kidd Creek VMS deposit, Ontario, Canada. Economic Geology and the Bulletin of the Society of Economic Geologists, 101, p.1055-1061.

Johnston, D.T., Wing, B.A., Farquhar, J., Kaufman, A.J., Strauss, H., Lyons, T.W., Kah, L.C., and Canfield, D.E., 2005. Active microbial sulfur disproportionation in the Mesoproterozoic. Science, 310, 1477-1479.

Kinnaird, J.A., Hutchinson, D., Schurmann, L., Nex, P.A.M., and de Lange, R., 2005. Petrology and mineralisation of the southern Platreef: northern limb of the Bushveld Complex, South Africa. Mineralium Deposita, 40, 576-597.

Manyeruke, T.D., Maier, W.D., and Barnes, S.-J., 2005. Major and trace element geochemistry of the Platreef on the farm Townlands, northern Bushveld Complex. South African Journal of Geology, 108, 381-396.

Mojzsis, S.J., Coath, C.D., Greenwood, J.P., McKeegan, K.D., and Harrison, T.M., 2003. Mass-independent isotope effects in Archean (2.5-3.8 Ga) sedimentary sulfides determined by ion microprobe analysis. Geochimica et Cosmochimica Acta 67, 1635-1658.

Naldrett, A.J., 2004, Magmatic sulfide deposits, Springer, New York. 727 pp.

Nex, P.A.M., Cawthorn, R.G., and Kinnaird, J.A., 2002. Geochemical effects of magma addition: compositional reversals and decoupling of trends in the Main Zone of the western Bushveld Complex. Mineralogical Magazine, 66, 833-856.

Ohmoto, H. and Rye, R.O., 1979, Isotopes of sulfur and carbon. In Geochemistry of hydrothermal ore deposits, 2nd ed. (Barnes, H.L., ed.), New York, 509-567.

Ono, S., Eigenbrode, J.L., Pavlov, A.A., Kharecha, P., Rumble, D., Kasting, J.F., and Freeman, K. H., 2003. New insights into Archean sulfur cycle from mass-independent sulfur isotope records from the Hamersley basin, Australia. Earth and Planetary Science Letters 213, 15-30.

Sakai, H., Des Marais, D.J., Ueda, A., and Moore, J.G., 1984. Concentrations and isotope ratios of carbon, nitrogen, and sulfur in ocean-floor basalts. Geochimica et Cosmochimica Acta, 48, 2433-2442.

Schiffries, C.M., and Rye, D.M., 1989. Stable isotopic systematics of the Bushveld Complex: I. Constraints of magmatic processes in layered intrusions. American Journal of Science, 289, 841-873.

Seal, II, R.R., 2006. Sulfur isotope geochemistry of sulfide minerals in Sulfide Mineralogy Geochemistry, Vaughan, D.J., ed., Reviews in Mineralogy and Geochemistry, 61. 633-677.

Sharman-Harris, E.R., Kinnaird, J.A., Harris, C., and Horstmann, U.E., 2005, A new look at sulphide mineralisation of the northern limb, Bushveld Complex: a stable isotope study. Applied Earth Science: Transactions of the Institute of Mining Metallurgy B. 114, B252-B263.

Torssander, P., 1989. Sulfur isotope ratios of Icelandic rocks. Contributions to Mineralogy and Petrology, 102. 18-23.

Thode, H.G., Monster, J., and Dunford, H.B., 1961. Sulfur isotope geochemistry. Geochimica et Cosmochimica Acta, 25. 159-174.

Viljoen, M.J., and Schürmann, L.W., 1998. Platinum-group metals. In: The Mineral Resources of South Africa (M.G.C. Wilson and C.R. Anhaeusser, eds.): Handbook, Council for Geoscience 16, 532-568.

Whitehouse, M.J., Kamber, B.S., Fedo, C.M., and Lepland, A., 2005. Integrated Pb- and S-isotope investigation of sulfide minerals from the early Archaean of southwest Greenland. Chemical Geology, 222, 112-131.

Table 1. Relatively pristine igneous rocks

Sample	Unit	$\delta^{33}S$	$\delta^{34}S$	$\delta^{36}S$	$\Delta^{33}S$	$\Delta^{36}S$
P3-MZLo	Main Zone	1.58	2.86	5.80	0.11	0.33
P3-MZHi	Main Zone	0.89	1.32	2.47	0.21	-0.05
N6.2	Main Zone	0.91	1.53	3.54	0.12	0.61
BHTv1.1	Main Zone	0.82	1.34	2.83	0.13	0.27
C2-20	Platreef	1.79	3.15	5.24	0.17	0.13

Note: $\Delta^{33}S=\delta^{33}S-1000*[(1+\delta^{34}S/1000)^{0.515}-1]$; $\Delta^{36}S=\delta^{36}S-1000*[(1+\delta^{34}S/1000)^{1.91}-1]$

Table 2: Unmetamorphosed equivalents of Platreef wall rocks

Sample	Stratigraphy	Lith.	$\delta^{33}S$	$\delta^{34}S$	$\delta^{36}S$	$\Delta^{33}S$	$\Delta^{36}S$
DF01-P	Duitschland	Shale	3.34	5.36	9.93	0.59	-0.28
DF02-P	Duitschland	Shale	0.66	-1.46	-4.73	1.41	-1.96
DF03-P	Duitschland	Shale	3.62	4.56	6.97	1.28	-1.71
DF04-P	Duitschland	Shale	3.23	3.99	5.98	1.18	-1.60
DF05-P	Duitschland	Shale	1.75	2.35	3.83	0.54	-0.64
DF08-C	Duitschland	Dol	14.25	27.58	53.13	0.14	0.09
DF09-C	Duitschland	Dol	14.1	27.2	52.43	0.18	0.13
DF10-C	Duitschland	Dol	14.21	27.7	53.43	0.04	0.14
DF13-C	Duitschland	Dol	12.42	24.11	46.19	0.08	-0.11
DF14-C	Duitschland	Dol	11.96	23.29	44.74	0.03	0.03
DF15-C	Duitschland	Dol	10.51	20.44	39.1	0.04	-0.09
DF16-C	Duitschland	Dol	8.31	16.14	30.71	0.03	-0.18
DF17-C	Duitschland	Ls	6.47	11.12	20.43	0.76	-0.80
DF18-C	Duitschland	Ls	3.37	6.17	11.59	0.2	-0.16
DF19-C	Duitschland	Dol	14.55	28.27	54.53	0.09	0.13
DF20-C	Duitschland	Dol	21.68	42.3	82.32	0.11	0.43
DF21-C	Duitschland	Dol	12.85	25.04	48.34	0.03	0.22
DF22-C	Duitschland	Dol	8.46	16.44	31.29	0.03	-0.18
DF23-C	Malmani	Dol	6.41	10.45	19.45	1.04	-0.50
DF26-C	Malmani	Dol	8.45	10.92	18.64	2.84	-2.20
DF27-C	Malmani	Dol	9.08	14.47	26.19	1.65	-1.49

Note: $\Delta^{33}S=\delta^{33}S-1000*[(1+\delta^{34}S/1000)^{0.515}-1]$; $\Delta^{36}S=\delta^{36}S-1000*[(1+\delta^{34}S/1000)^{1.90}-1]$

Table 3. Coexisting sulfides

Sample	Description	$\delta^{33}S$	$\delta^{34}S$	$\delta^{36}S$	$\Delta^{33}S$	$\Delta^{36}S$
P1-56A	Po	3.18	5.92	11.67	0.13	0.33
P1-56B	Ccp	3.51	6.65	12.62	0.09	-0.11
G1-102A	Po/Pnt	2.60	4.64	8.22	0.21	0.28
G1-102B	Ccp	4.65	8.58	14.88	0.24	-0.65
G1-102C	Sulf	2.34	4.05	6.76	0.26	-0.06
P2-228A	Po/Pnt	6.65	12.70	24.08	0.13	-0.32
P2-228B	Ccp	5.98	11.44	22.03	0.10	0.05
P5-310a	Po	3.12	5.87	11.31	0.10	0.06
P5-310b	Po	3.13	5.84	11.28	0.12	0.10
P5-310c	Ccp	3.24	6.06	11.91	0.12	0.31
C1-19a	Po	4.75	8.39	15.57	0.44	-0.51
C1-19b	Po	4.86	8.68	16.46	0.40	-0.18
C1-19c	Ccp	3.95	7.19	13.45	0.25	-0.33
C1-18a	Po	4.73	8.36	15.75	0.43	-0.28
C1-18b	Po	4.74	8.36	15.64	0.44	-0.38
C1-18c	Ccp	4.86	8.60	16.13	0.44	-0.36

Note: $\Delta^{33}S=\delta^{33}S-1000*[(1+\delta^{34}S/1000)^{0.515}-1]$; $\Delta^{36}S=\delta^{36}S-1000*[(1+\delta^{34}S/1000)^{1.91}-1]$

Table 4. Core C1

Sample	Depth (m)	Lithology	$\delta^{33}S$	$\delta^{34}S$	$\delta^{36}S$	$\Delta^{33}S$	$\Delta^{36}S$
5	49.6	Feldspathic Pyroxenite	2.32	4.01	7.69	0.26	0.02
11	102.8	Feldspathic Pyroxenite	4.66	8.77	16.59	0.15	-0.23
14	131.5	Feldspathic Pyroxenite	4.96	9.20	17.71	0.23	0.06
16a	144.8	Feldspathic Pyroxenite	4.04	6.94	12.80	0.47	-0.49
18	147.1	Feldspathic Pyroxenite	4.77	8.44	15.84	0.44	-0.34
19	148.7	Feldspathic Pyroxenite	4.84	8.34	15.89	0.55	-0.10
20	149.6	Feldspathic Pyroxenite	4.79	8.45	15.99	0.45	-0.21
21	150.8	Feldspathic Pyroxenite	4.73	8.24	15.68	0.49	-0.12
22	151.5	Feldspathic Pyroxenite	4.52	8.17	15.29	0.32	-0.37
23	159.1	Calc-silicate	1.02	0.72	0.96	0.65	-0.42
25	169.9	Calc-silicate	5.62	8.23	15.46	1.39	-0.32
25a	171.6	Calc-silicate	3.73	4.62	8.48	1.35	-0.37
25b	174.8	Calc-silicate	5.08	5.77	9.94	2.11	-1.11
25c	177.3	Calc-silicate	6.11	5.29	7.61	3.39	-2.52
26	179.3	Calc-silicate	6.92	4.88	5.20	4.41	-4.13
27	185.5	Calc-silicate	8.15	6.07	7.21	5.04	-4.41
31	214.6	Calc-silicate	7.81	6.71	9.08	4.36	-3.77
38	301.9	Calc-silicate	6.23	5.60	7.98	3.35	-2.74

Note: $\Delta^{33}S=\delta^{33}S-1000*[(1+\delta^{34}S/1000)^{0.515}-1]$; $\Delta^{36}S=\delta^{36}S-1000*[(1+\delta^{34}S/1000)^{1.91}-1]$

Table 5. Core P1

Sample	Depth (m)	Lithology	$\delta^{33}S$	$\delta^{34}S$	$\delta^{36}S$	$\Delta^{33}S$	$\Delta^{36}S$
74	130.2	Pyroxenite	1.93	3.44	6.30	0.16	-0.28
167	196.0	Feldspathic Pyroxenite	2.18	3.78	6.62	0.23	-0.61
109	206.2	Pyroxenite	1.61	3.07	5.16	0.03	-0.72
139	314.7	Pyroxenite	1.56	2.74	5.17	0.15	-0.07
22	331.3	Pyroxenite	2.50	4.54	7.04	0.16	-1.64
2-2	335.0	Pyroxenite	3.56	6.73	11.93	0.09	-0.97
56A	336.9	Pyroxenite	3.14	5.86	10.78	0.13	-0.43
56B	336.9	Pyroxenite	3.47	6.59	11.74	0.09	-0.88
2-1	338.2	Leuconorite	5.31	10.14	19.25	0.10	-0.21
149	343.9	Serpentinized Pyroxenite	5.97	11.40	22.05	0.12	0.15
H1	345.6	Hornfels	9.62	18.10	35.11	0.34	0.26
P2	350.1	Calc-silicate	3.29	6.08	10.97	0.17	-0.67
H2	352.8	Hornfels	-0.53	-1.08	-2.95	0.03	-0.89
H3	353.6	Hornfels	0.11	0.04	-1.15	0.09	-1.24
H6	366.2	Hornfels	-0.02	-0.85	-3.44	0.41	-1.83
H7	373.9	Hornfels	0.00	-0.67	-3.35	0.35	-2.07
H8	374.9	Hornfels	0.24	-0.26	-2.60	0.38	-2.11
H9a	381.8	Hornfels	-7.31	-14.47	-26.34	0.17	1.11
H9c	392.5	Hornfels	1.03	0.59	-0.93	0.72	-2.06
H10	395.4	Hornfels	1.73	1.57	0.22	0.93	-2.78
B1	409.4	BIF	8.90	15.83	29.58	0.78	-0.87
B2	414.6	BIF	3.03	4.40	7.29	0.77	-1.12

Note: $\Delta^{33}S=\delta^{33}S-1000*[(1+\delta^{34}S/1000)^{0.515}-1]$; $\Delta^{36}S=\delta^{36}S-1000*[(1+\delta^{34}S/1000)^{1.91}-1]$

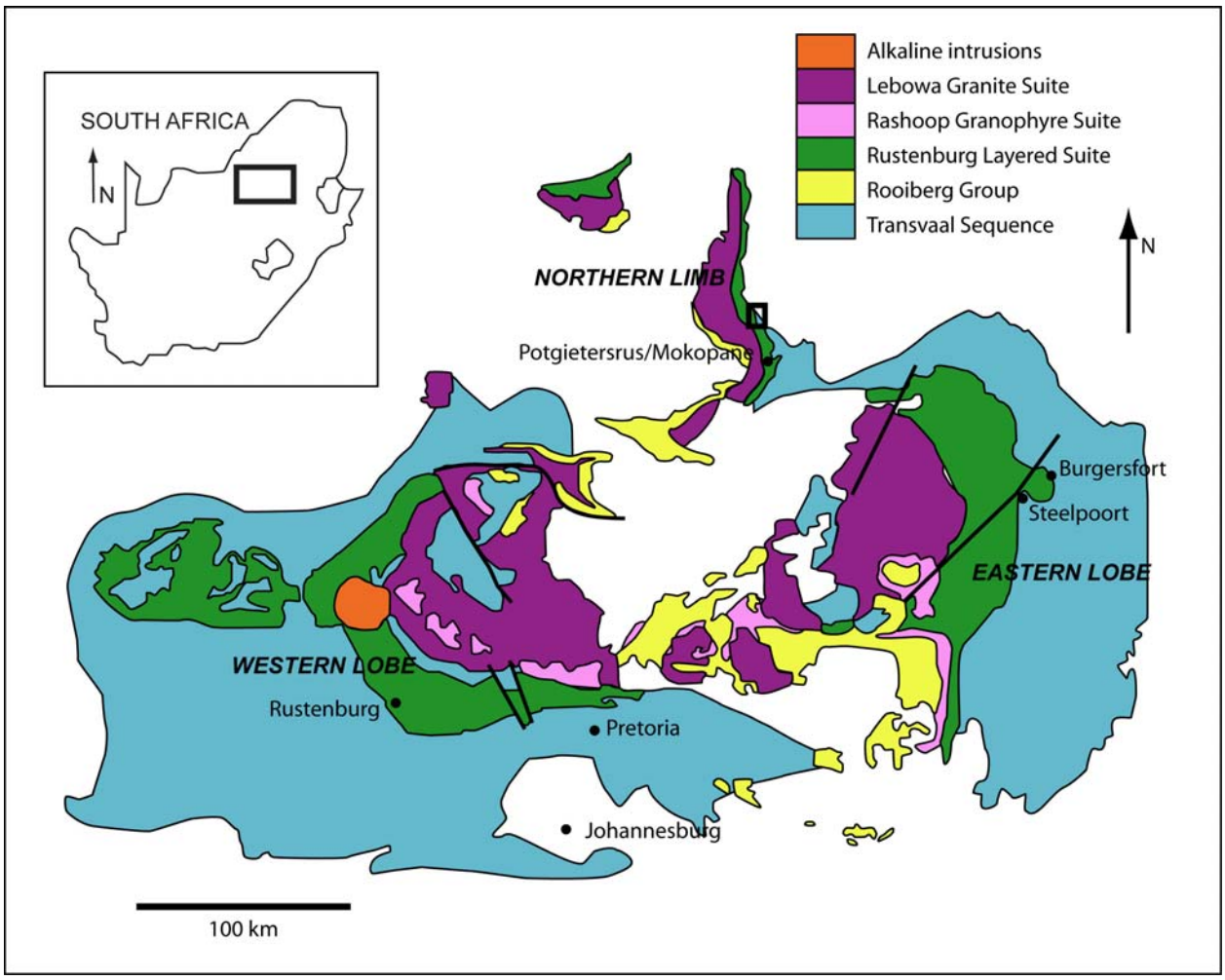

Figure 1. Geological sketch map of the Bushveld Complex (after Kinnaird *et al.*, 2005). Different colors indicate major units in the Bushveld igneous stratigraphy. Map does not differentiate the southern (Bethal) limb, which is a minor ~ 10 km by 40 km structure trending N-S in the southeast corner of the Bushveld. The Platreef is located north of the city of Mokopane (Potgietersrus) in the Mokopane (Potgietersrus) Limb.

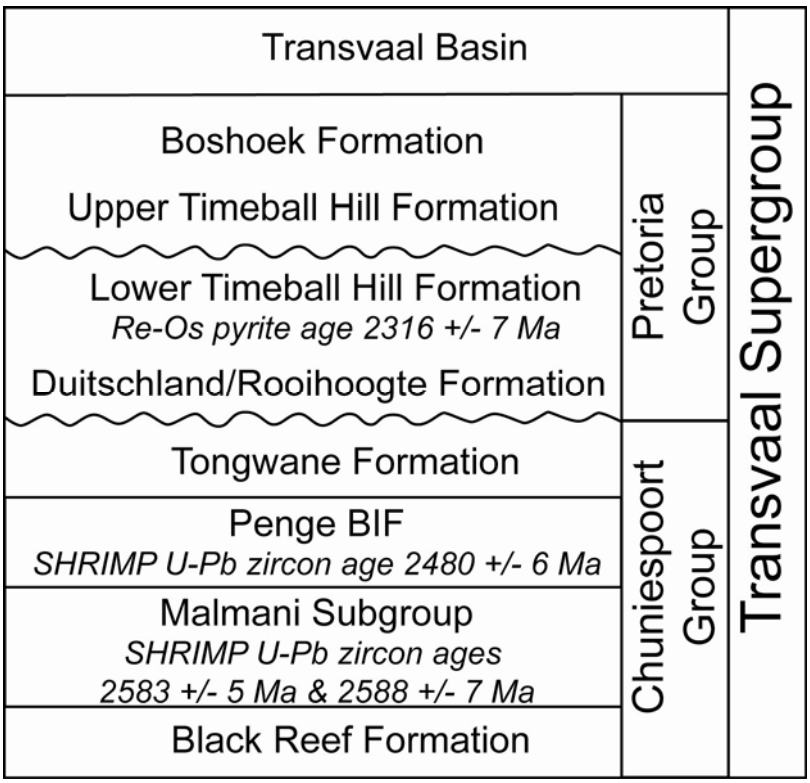

Figure 2. Stratigraphic column of the Transvaal Supergroup sedimentary rocks (after Bekker *et al.*, 2004; Hannah *et al.*, 2004).

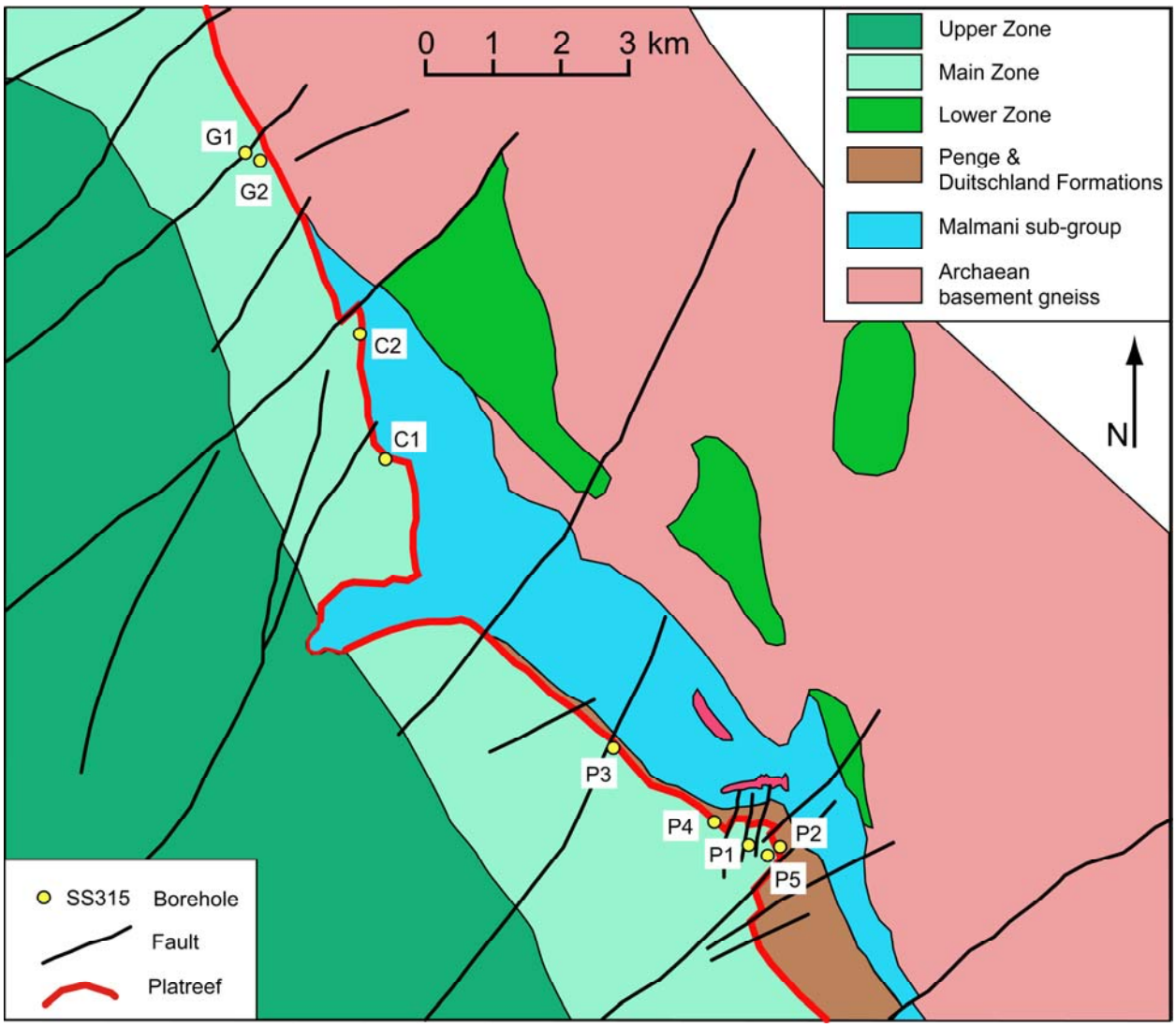

Figure 3. Detailed geologic sketch map of the region in the box in Figure 1. Borehole locations for samples analyzed for sulfur isotope composition are indicated by yellow circles.

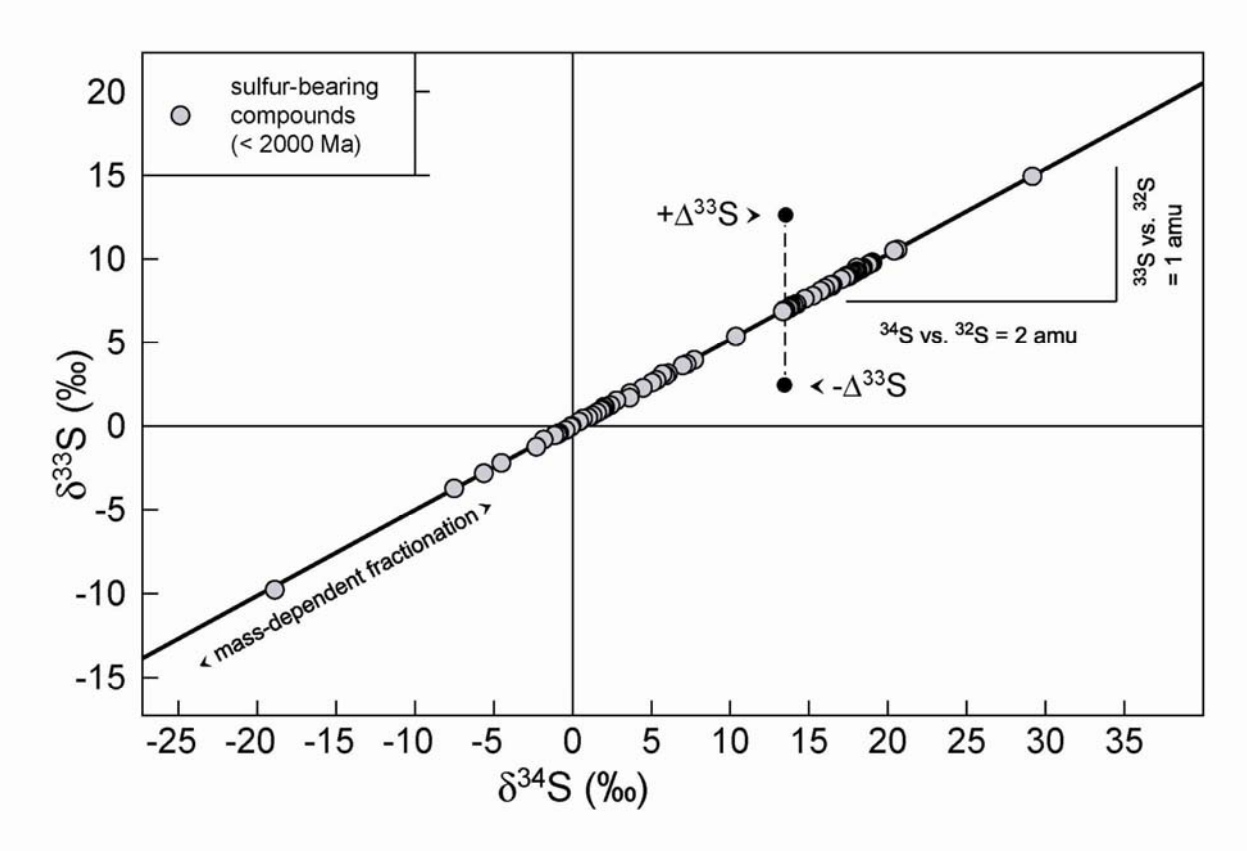

Figure 4. Mass-dependent fractionation line of $\delta^{34}S$ vs. $\delta^{33}S$. Most terrestrial processes involve mass-dependent fractionation of sulfur isotopes which fall on a line with slope of ~0.515. Deviations from mass-dependent fractionation are expressed as non-zero values of $\Delta^{33}S$.

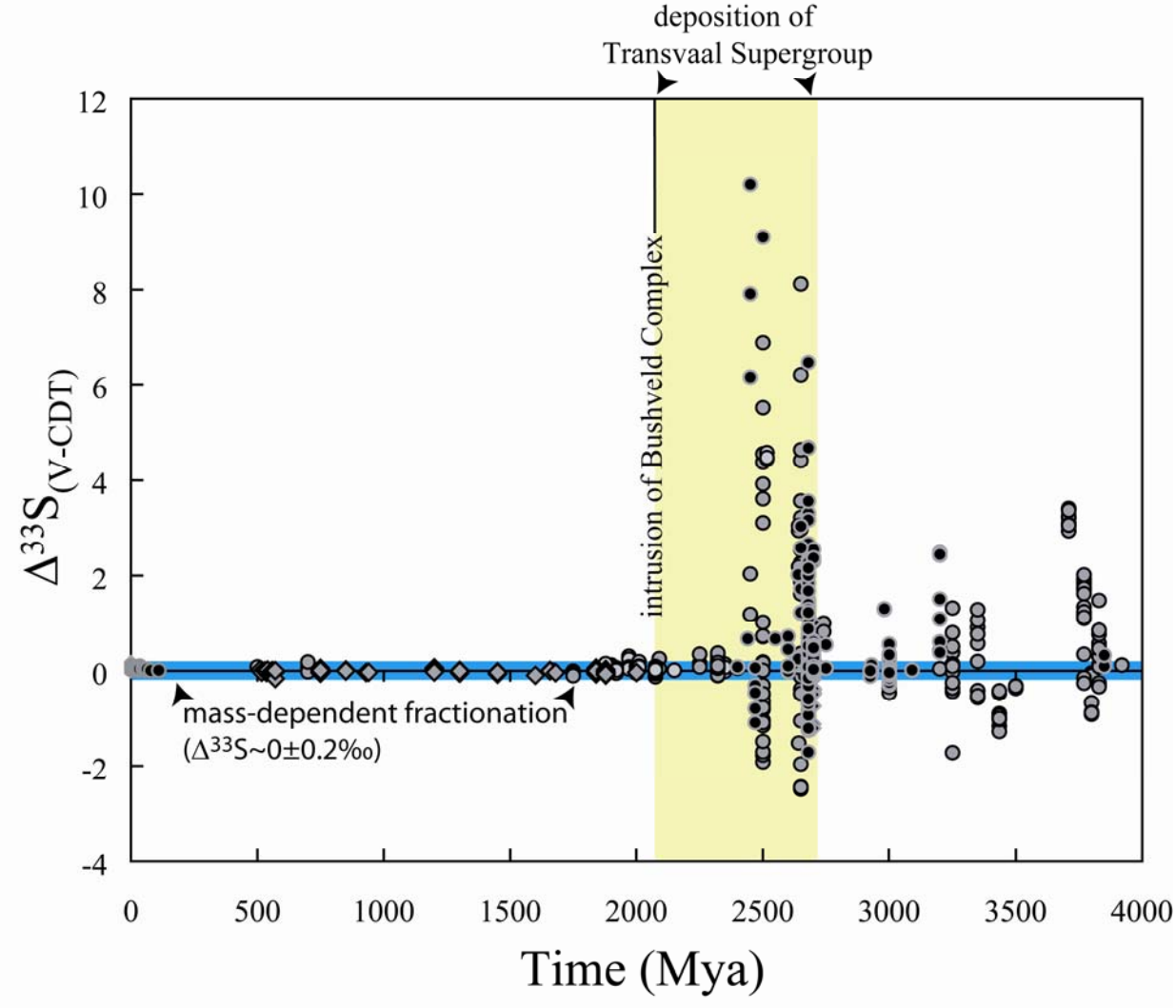

Figure 5. Compilation of $\Delta^{33}S$ over time from Farquhar *et al.* (2000, 2002), Mozjsis *et al.* (2003), Ono *et al.* (2003), Hu *et al.* (2003), Bekker *et al.* (2004), Johnston *et al.* (2005), Whitehouse *et al.* (2005), unpublished data (UMD). The time period for deposition of wall rocks surrounding the Bushveld (Transvaal Supergroup) is indicated along with the intrusion of the Bushveld Complex.

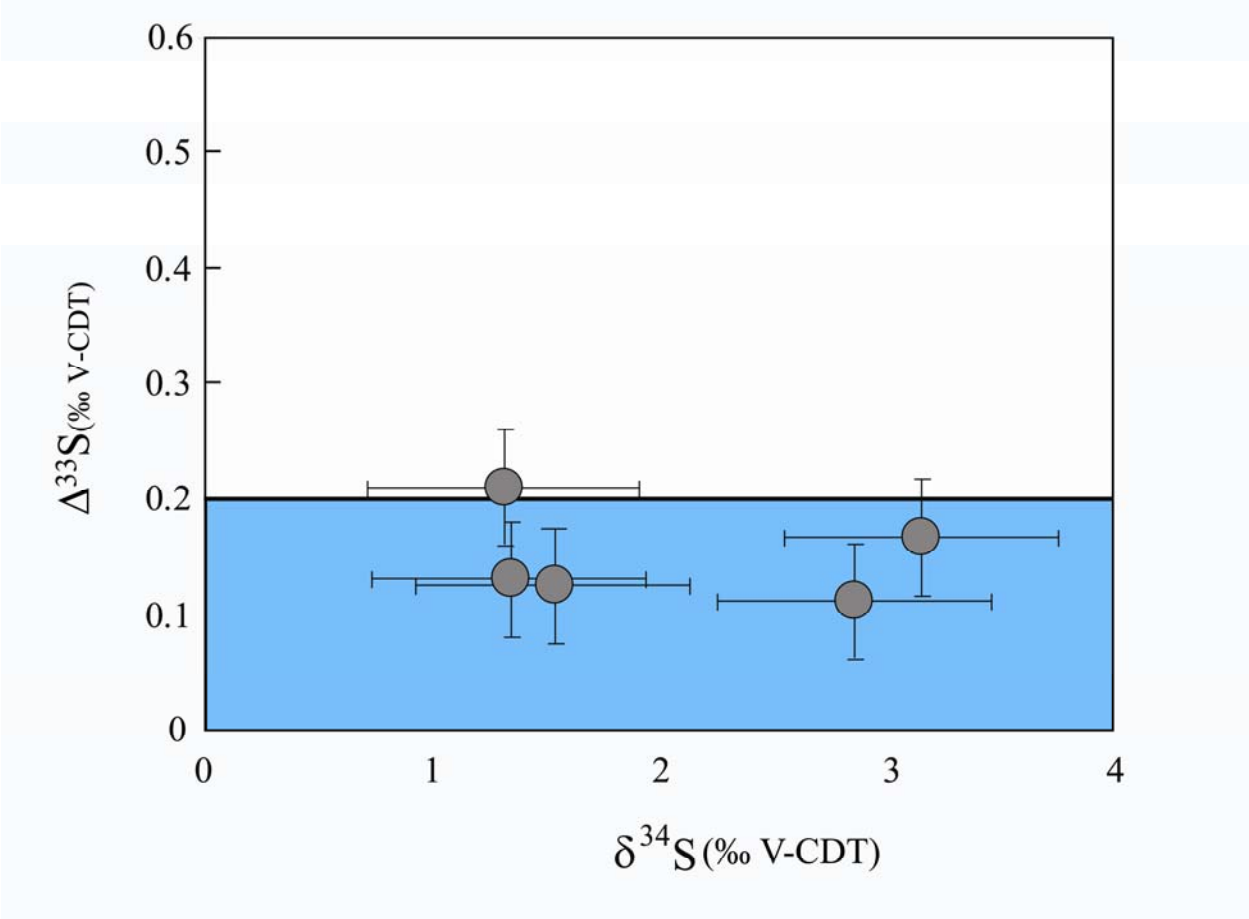

Figure 6. Sulfur isotope composition of relatively pristine igneous rocks. Light blue box shows the upper limit of mass-dependent value of $\Delta^{33}S$.

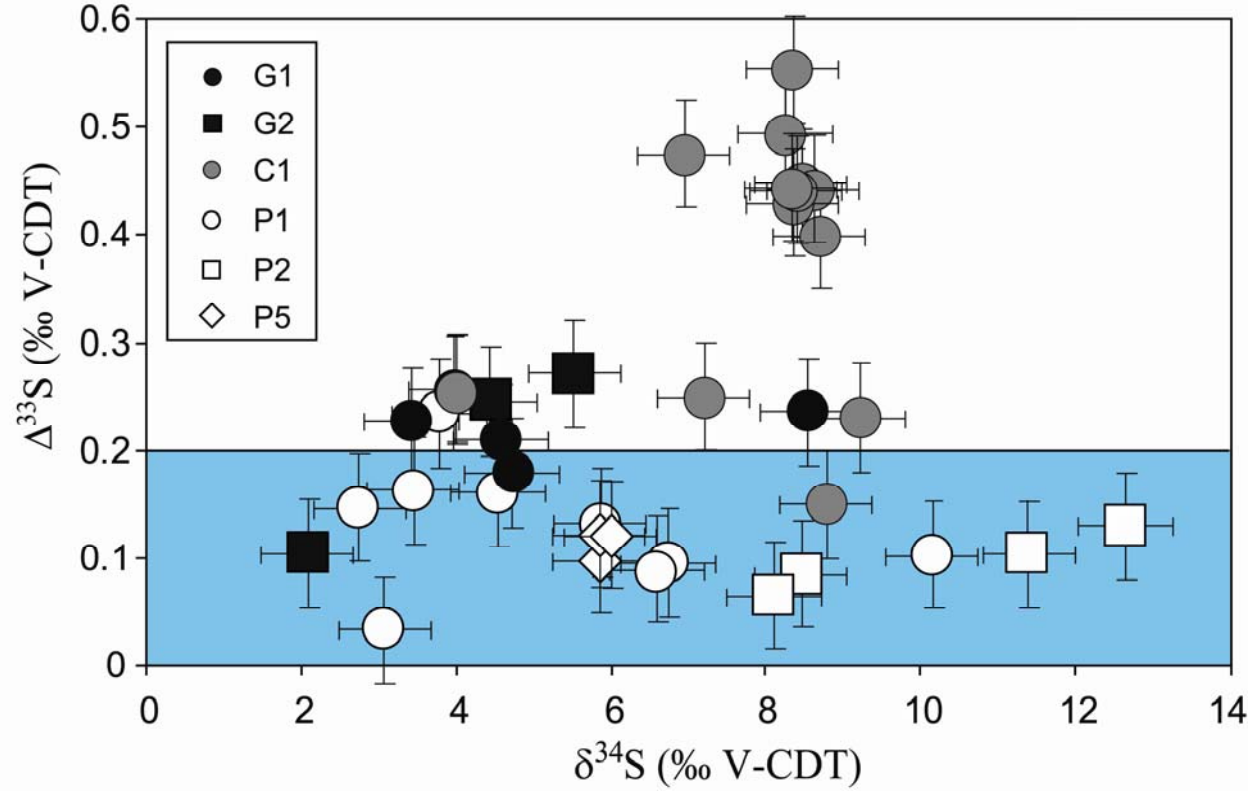

Figure 7. Plot of sulfur isotope composition of samples from the Platreef ore horizon. Samples from six different cores are shown (See map in Figure 5 for borehole locations). Error bars for $\delta^{34}S$ are approximately the size of the symbol. Several samples record mass-independent sulfur isotope compositions (plot outside of error of the range of mass-dependent values, $\Delta^{33}S \leq 0.2‰$). Light blue box shows the upper limit of mass-dependent value of $\Delta^{33}S$.

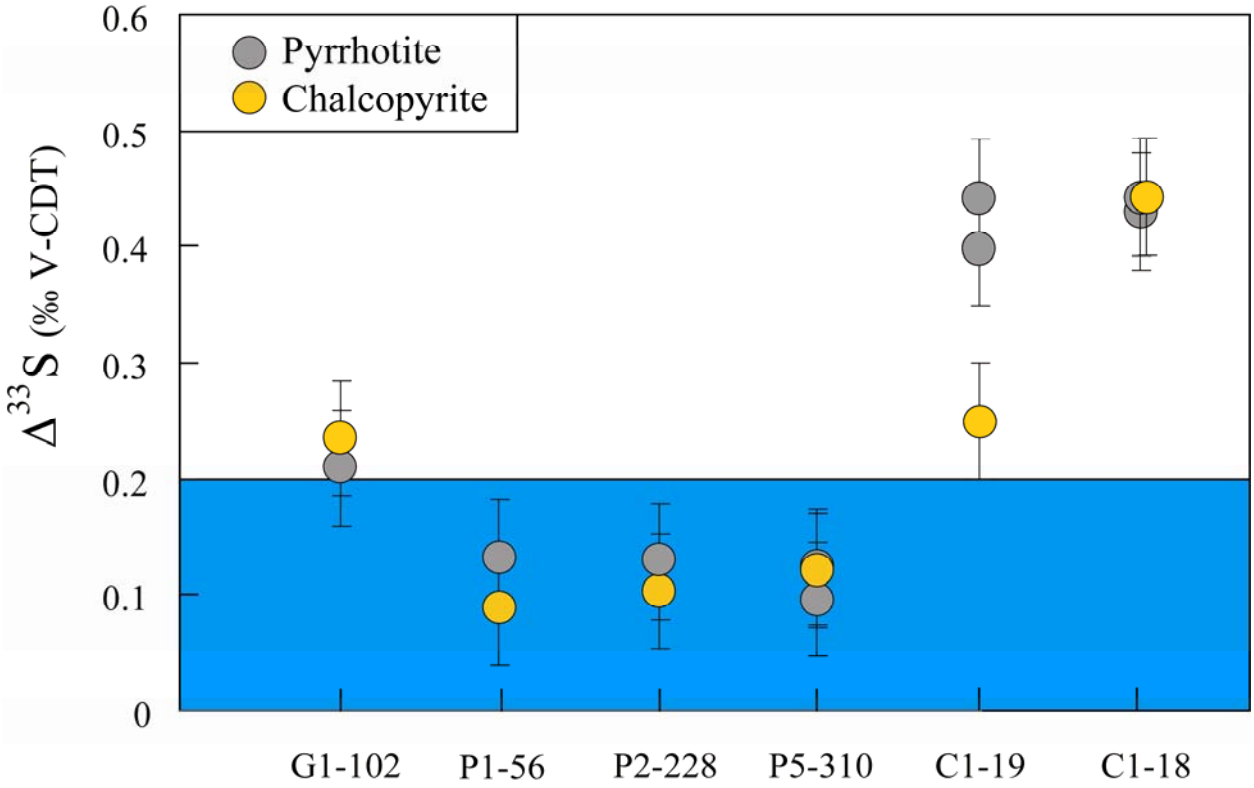

Figure 8. Sulfur isotope ($\Delta^{33}S$) compositions of coexisting sulfides in six different samples. In all but one sample (C1-19) $\Delta^{33}S$ is the same within error of measurement for all sulfides analyzed. Pyrrhotite fractions were split into two and run separately to check for accuracy of separation in three of the samples (P5-310, C1-19, C1-18). Light blue box shows the upper limit of mass-dependent value of $\Delta^{33}S$.

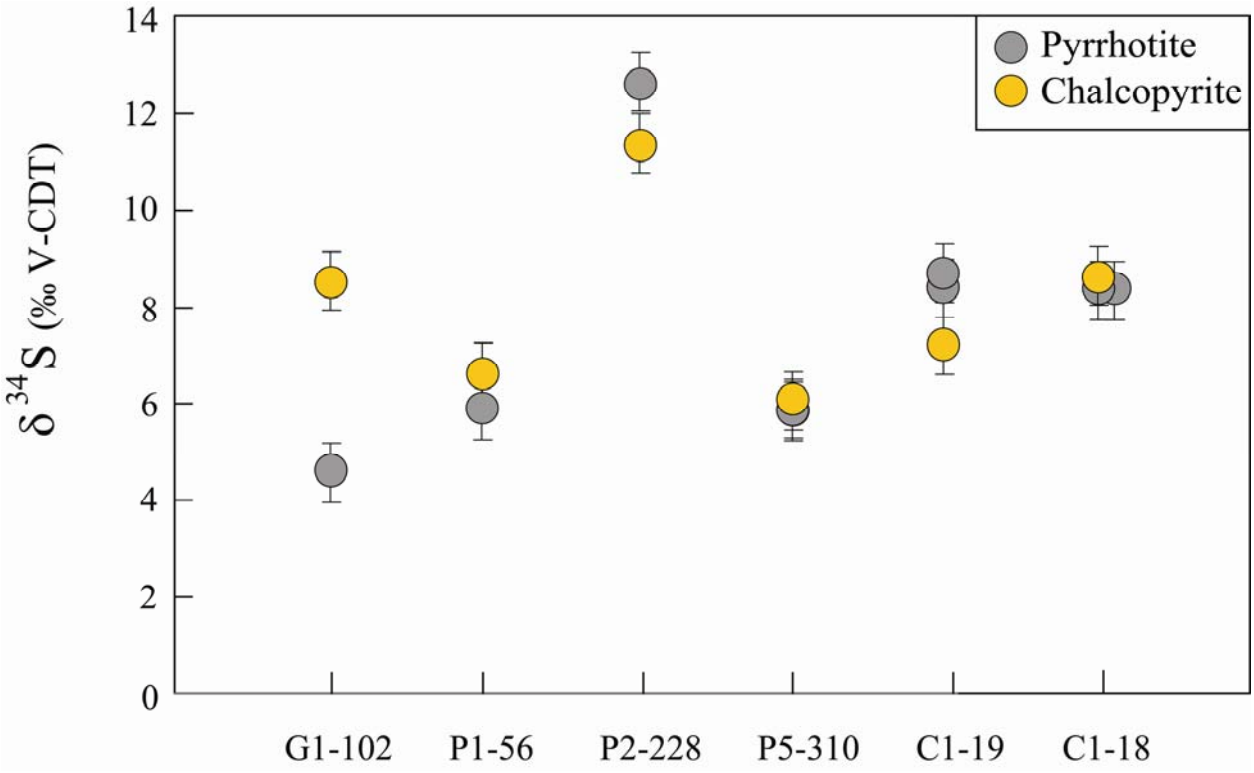

Figure 9. Sulfur isotope compositions of coexisting sulfides in six different samples. Experimental data suggest that at equilibrium $\delta^{34}S_{Ccp} < \delta^{34}S_{Po}$ (Ohmoto and Rye, 1979). This relationship is observed for two of the samples (P2-228 and C1-19), however sample G1-102 exhibits the reverse relationship. Pyrrhotite fractions were split into two and run separately to check for accuracy of separation in three of the samples (P5-310, C1-19, C1-18).

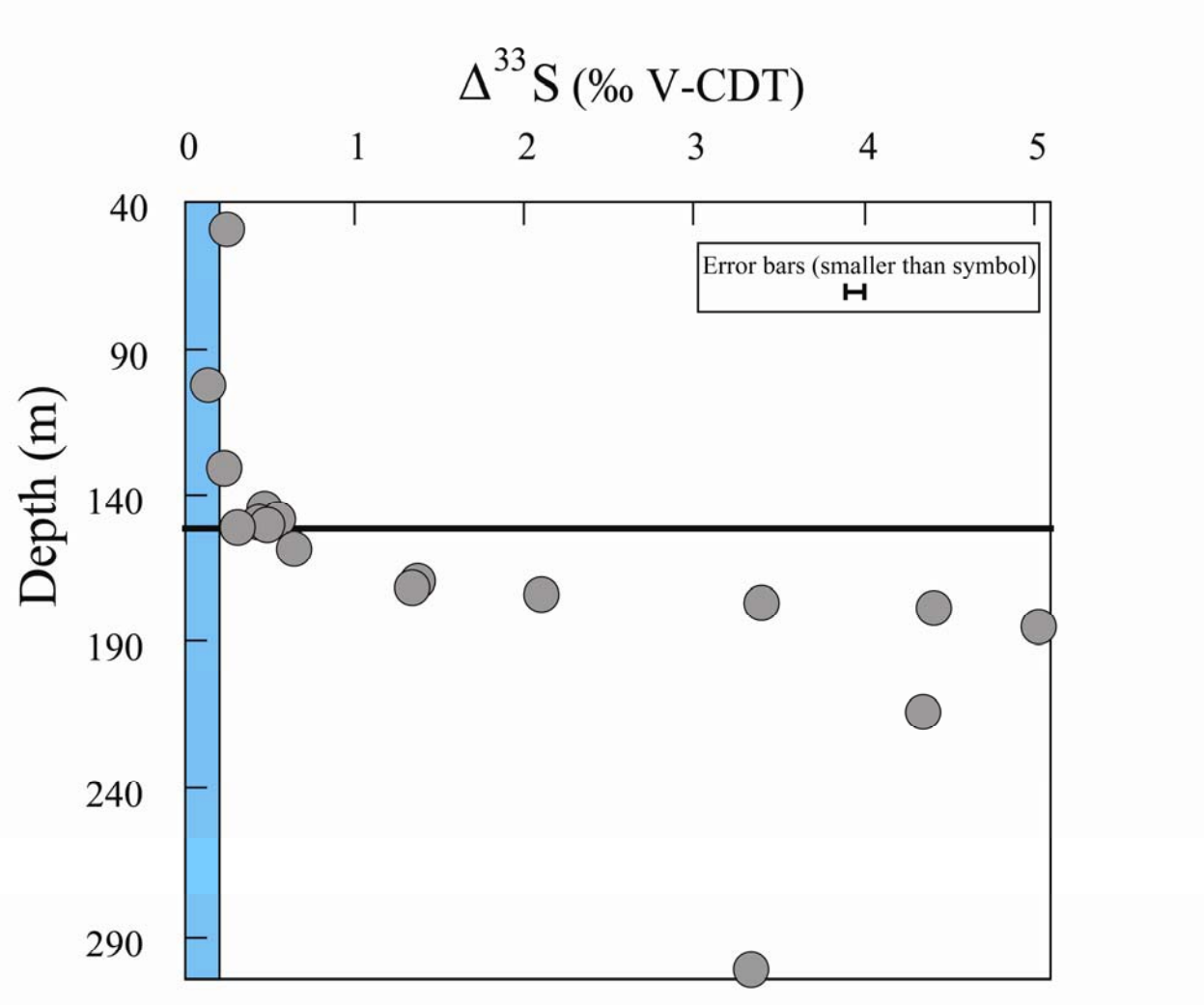

Figure 10. Δ^{33}S composition of samples in C1 carbonate core. Upper part of graph is igneous rock of Platreef. Line at 151 m is the contact between Platreef and underlying wall rocks. Error bars (2σ) of Δ^{33}S measurements are the size of the symbols. Light blue box shows the upper limit of mass-dependent value of Δ^{33}S.

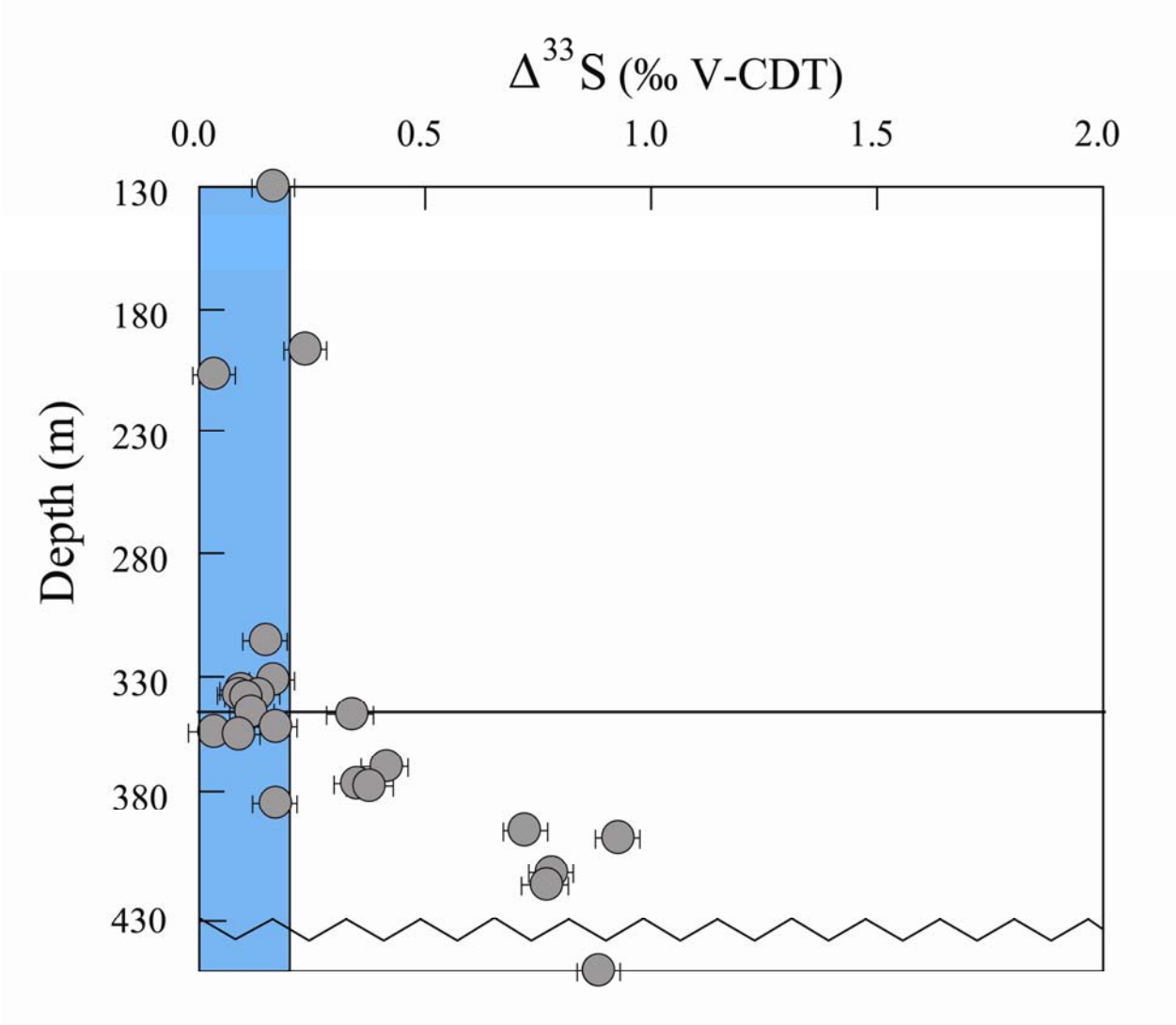

Figure 11. Δ^{33}S composition of samples in P1 pelite core. Upper part of graph is igneous rock of Platreef. Line at 344 m is the contact between Platreef and underlying wall rocks. Light blue box shows the upper limit of mass-dependent value of Δ^{33}S.

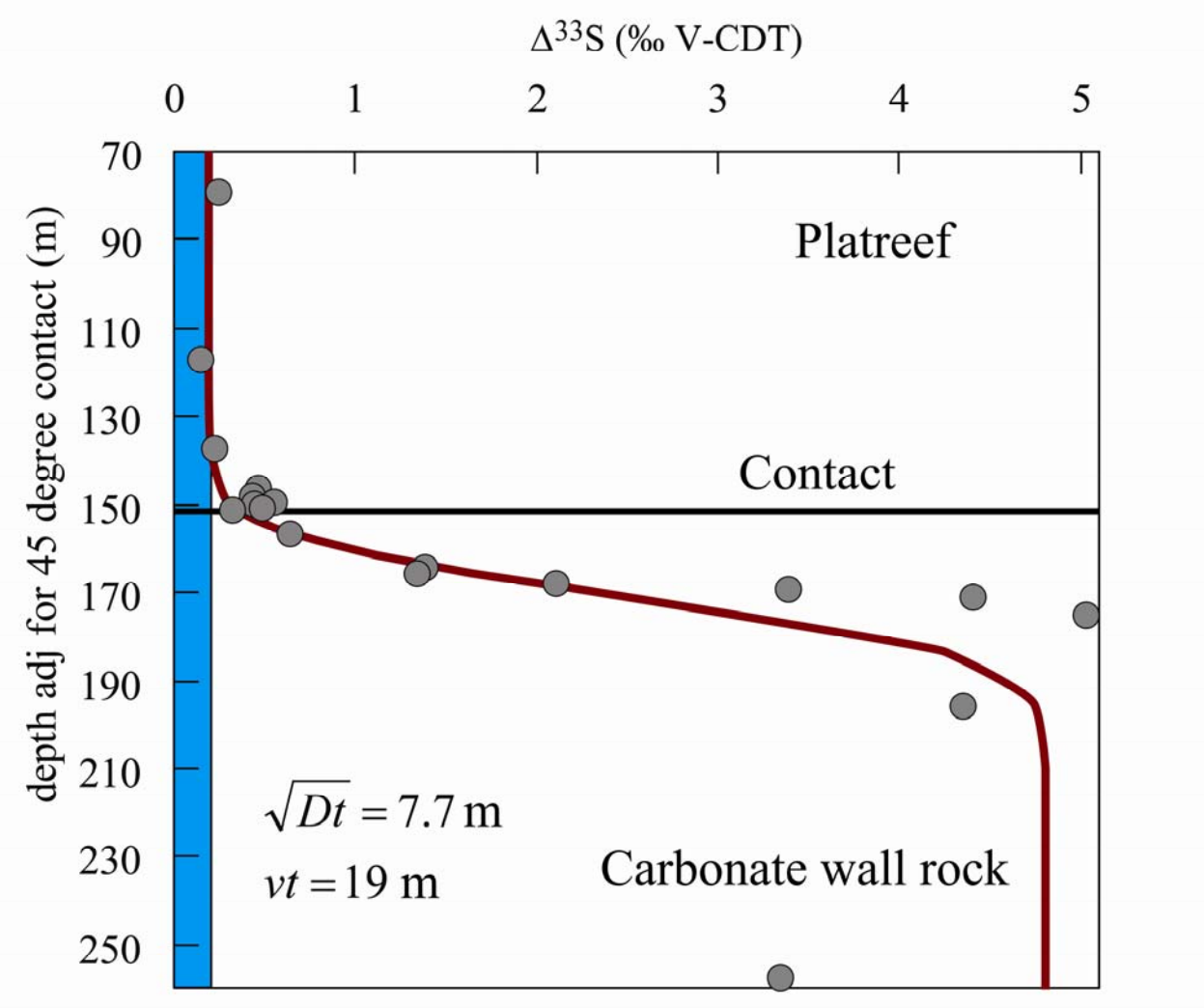

Figure 12. Sulfur isotope compositions of core C1 with depth adjusted for 45 degree angle contact between Platreef and carbonate wall rock. Dark red line is best fit to data using solution to the mass continuity equation. Diffusive distance $\sqrt{Dt}$ and advective distance (vt) are derived from the solution. Error bars (2σ) of $\Delta^{33}S$ measurements are the size of the symbols. Light blue box shows the upper limit of mass-dependent value of $\Delta^{33}S$.

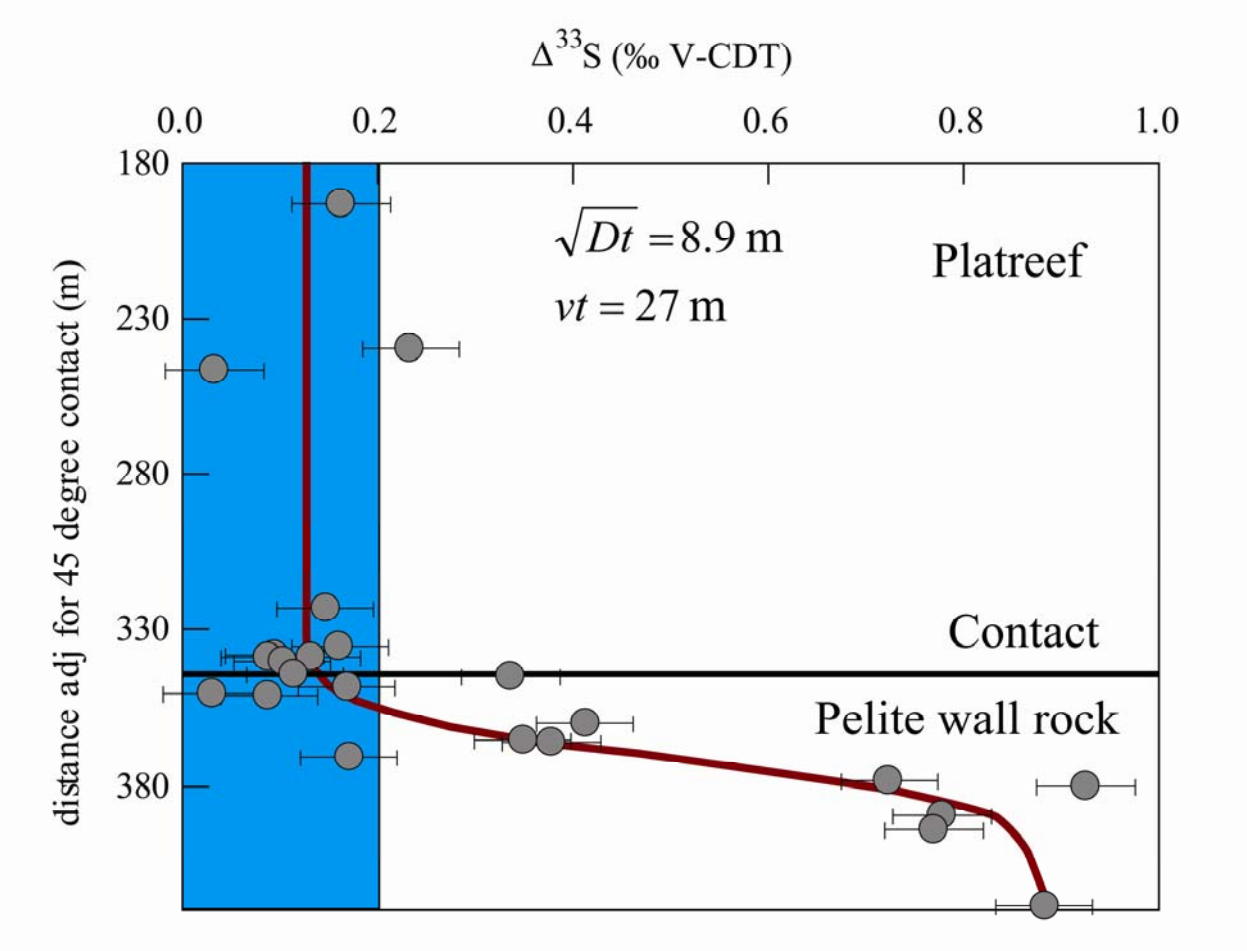

Figure 13. Sulfur isotope compositions of core P1 with depth adjusted for 45 degree angle contact between Platreef and wall rock. Dark red line is best fit to data using solution to the mass continuity equation. Diffusive distance $\sqrt{Dt}$ and advective distance (vt) are derived from the solution. (Error bars are 2σ) Light blue box shows the upper limit of mass-dependent value of $\Delta^{33}S$.